International Journal of
MATERIALS RESEARCH

Zeitschrift für METALLKUNDE

Original Contributions

Arijit Laik[a], Karanam Bhanumurthy[b], Gajanan Balaji Kale[a,c], Bhagwati Prasad Kashyap[d]
[a] Materials Science Division, Bhabha Atomic Research Centre, Mumbai, India
[b] Scientific Information Resource Division, Bhabha Atomic Research Centre, Mumbai, India
[c] Presently retired from Materials Science Division, Bhabha Atomic Research Centre.
[d] Department of Metallurgical Engineering and Materials Science, Indian Institute of Technology Bombay, Mumbai, India

Diffusion characteristics in the Cu–Ti system

The formation and growth of intermetallic compounds by diffusion reaction of Cu and Ti were investigated in the temperature range 720–860 °C using bulk diffusion couples. Only four, out of the seven stable intermediate compounds of the Cu–Ti system, were formed in the diffusion reaction zone in the sequence CuTi, Cu_4Ti, Cu_4Ti_3 and $CuTi_2$. The activation energies required for the growth of these compounds were determined. The diffusion characteristics of Cu_4Ti, CuTi and Cu_4Ti_3 and Cu(Ti) solid solution were evaluated. The activation energies for diffusion in these compounds were 192.2, 187.7 and 209.2 kJ mol^{-1} respectively, while in Cu(Ti), the activation energy increased linearly from 201.0 kJ mol^{-1} to 247.5 kJ mol^{-1} with increasing concentration of Ti, in the range 0.5–4.0 at.%. The impurity diffusion coefficient of Ti in Cu and its temperature dependence were also estimated. A correlation between the impurity diffusion parameters for several elements in Cu matrix has been established.

Keywords: Diffusion reaction; Intermetallics; Solid-state reaction; Kinetics; Activation energy

1. Introduction

Copper–titanium alloys find places in various engineering applications such as high strength springs, electrical contacts and diaphragms, due to their high yield strength, generally exceeding 700 MPa in age-hardened condition [1]. These alloys also exhibit outstanding corrosion and wear resistance and are hence used extensively in bio-medical applications [2]. Cu–Ti alloys, due to their metallization capability, are also used in brazing ceramics, such as polycrystalline alumina [3]. The Cu–Ti system has been investigated extensively [1–14] with the primary interest being phase transformations of various kinds [1, 4–6].

Despite the fact that diffusion plays an important role in these phase transformations and determines the final properties of the Cu–Ti alloys, only a few studies have focused on evaluation of diffusion properties of this system [7–9]. Rexer [7] reported the intrinsic diffusion coefficient of Ti in Cu-1.1 and 4.1 at.% Ti alloys at 800 and 900 °C, based on their experiments on boronizing of these alloys. Iijima et al. [9] evaluated the impurity diffusion coefficient of Ti in Cu and interdiffusion coefficient in a narrow concentration range 0–1.5 at.%Ti. Taguchi et al. [8] observed that six layers of intermetallic compounds formed by the diffusion reaction between Cu and Ti in the temperature range 690–870 °C, but reported the diffusion coefficients of only Cu_4Ti_3 and CuTi. Nevertheless, the diffusion behaviour of the entire Cu(Ti) terminal solid solution, which is decisive in determining the properties of the commercially used dilute Cu–Ti alloys, remains unaddressed. Moreover, diffusion also plays a major role in precipitation and growth of the metastable β′- and stable β-Cu_4Ti phases in these alloys via the process of spinodal decomposition [1, 5, 15–17], but no report on the diffusion properties of Cu_4Ti is available in the literature.

A number of studies have also been directed towards diffusion reaction of Cu and Ti [8, 10–12]. While Taguchi et al. [8] reported the formation of six intermetallic compounds in the Cu–Ti bulk diffusion couple, Oliker et al. [10] observed only five under similar conditions. Thin film experiments by Liotard et al. [12] revealed that the first phase to form at the Cu/Ti interface is CuTi, followed by

the metastable Cu_3Ti in the temperature range 300–475 °C, while Gershinskii et al. [11] reported the formation of Cu_7Ti_2, CuTi and $CuTi_2$ intermetallic compounds in thin film couples in the range 450–650 °C.

The Cu–Ti reactivity is of significant commercial importance. For example, during the brazing of Ti using Cu–Ag alloy, the reactivity between Cu and Ti is crucial in achieving sound joints. Recently, Andrieux et al. [13] observed that four interfacial reaction layers of Cu_4Ti, Cu_4Ti_3, CuTi and $CuTi_2$ form between Ti and the Cu–Ag alloy which is in concurrence with the observations of Shiue et al. [14] during infrared brazing of Cu and Ti. Attempts to develop coatings of Cu-Ti intermetallic compounds on Cu-substrate, led to the formation of Cu_4Ti and $CuTi_2$ in the coating layers by diffusion reaction [18]. Hence, a general agreement on diffusion reaction of the Cu–Ti system does not emerge from the reported literature.

Recently the Cu–Ti binary phase diagram has also undergone significant modifications on the Ti-rich side [19]. Following a revised thermodynamic assessment of the system by Canale and Servant [20], $CuTi_3$ was included in the six stable intermediate compounds; viz., Cu_4Ti, Cu_2Ti, Cu_3Ti_2, Cu_4Ti_3, CuTi and $CuTi_2$ that existed in the earlier phase diagram [21].

The objective of the present study was to provide an insight into the diffusion reaction between Cu and Ti, to determine the sequence of formation of the product phases and to elucidate the diffusion characteristics of the Cu–Ti system. The activation energies for the growth of intermetallic compounds formed in the diffusion zone were determined. The diffusion coefficients and activation energy for interdiffusion in these compounds, Cu(Ti) terminal solid solution and impurity diffusion of Ti in Cu were also evaluated.

2. Experimental procedure

2.1. Preparation of diffusion couples

Copper of 99.9 wt.% purity (OFHC grade) and titanium of 99.9 wt.% purity, in the form of 10 mm × 10 mm × 4 mm pieces were used to prepare bulk diffusion couples. The Cu and Ti pieces were sealed in separate quartz capsules under He atmosphere and pre-annealed for 48 h at 900 °C and 1000 °C, respectively, to obtain a strain-free and coarse grained structure. The joining surfaces of Cu and Ti pieces were mechanically polished to a surface finish of 1 μm. These pieces were cleaned ultrasonically with acetone and then immediately coupled under compressive stress in a vacuum hot-press. A compressive stress of 5 MPa and vacuum level better than 10^{-5} mbar was maintained throughout the diffusion-bonding operation. Mica sheets were used as spacers on either side of the couple, to prevent contact with the graphite ram of the hot-press. The couples were bonded at a temperature of 850 °C for 0.5 h and were then furnace cooled. It may be mentioned here that formation of TiC on the exposed surface of Ti-pieces during bonding, requires a partial pressure of CO, $p_{CO} \geq 10^{-4}$ mbar, according to the equilibrium thermodynamics of the Ti–C–O system [22]. However, since the prevailing partial pressure under dynamic vacuum, $p_{CO} \approx 10^{-6}$ mbar, was two orders of magnitude lower than the equilibrium value, it may be safely inferred that the possibility of formation of TiC is remote. The fact that the Ti pieces did not lose their metallic lustre even after the diffusion bonding, confirmed that TiC was not formed. Preliminary chemical analysis of the as-bonded couples using electron probe microanalysis (EPMA) across the interface showed excellent contact with a negligible diffusion width.

2.2. Diffusion annealing of the couples

The diffusion bonded couples were sealed in quartz capsules under He atmosphere, at a residual pressure of 1.5 kPa. The sealed diffusion couples were annealed at different temperatures in the range of 720–860 °C for 120 h each, in a pre-heated horizontal resistance heating tubular furnace. The temperature of the furnace was controlled within ±1 °C, using a proportional type temperature controller. The thermocouple used for temperature measurement was calibrated before the heat treatment and its tip was kept very close to the diffusion couple. The heat treatment schedule is given in Table 1. On completion of the diffusion annealing, the couples were quenched in water.

2.3. Characterization of the diffusion zones

After annealing, the diffusion couples were sectioned parallel to the diffusion direction using a slow speed diamond saw. The cross-sections of the couples were metallographically prepared to a surface finish of 0.25 μm and etched with a solution of H_2O, HNO_3 and HF in a proportion of 10 : 9 : 1 by volume. The cross-sections of the couples were characterized by using an optical microscope

Table 1. Experimental conditions for diffusion annealing of the Cu–Ti diffusion couples and the thicknesses of the phases formed in the diffusion zone.

Couple No.	Temperature (°C)	Time (h)	Thicknesses of the phases formed (in μm)				
			Cu_4Ti	Cu_4Ti_3	CuTi	$CuTi_2$	β-Ti
1.	720	120	16	5	25	*	#
2.	750	120	18	7	35	*	#
3.	780	120	23	8	46	1	8
4.	800	120	26	9	52	2	50
5.	830	120	38	12	56	3	240
6.	860	120	40	14	62	4	520

* Does not form continuous layer, # Does not form.

and an EPMA equipped with wavelength dispersive spectrometers (WDS). A stable electron beam with 20 kV accelerating voltage and beam current of 40 nA was used. The microstructures of the diffusion zones were recorded using secondary electron (SE) and back-scattered electron (BSE) imaging. Pure elemental standards of Cu and Ti were used for calibration and lithium fluoride (LiF) crystals were used for diffraction of Cu-K_α and Ti-K_α X-ray lines in the spectrometers, during quantitative analysis. The standard PAP correction program [23] was used for atomic number (Z), absorption (A) and fluorescence (F) corrections. Quantitative analysis on a point-to-point basis was done at regular intervals of 1–2 μm, by scanning the sample across the diffusion zones, to determine the concentration profile. For each point, the X-ray signals were counted for 20 s at the peak positions and 10 s each for the positive and negative background positions for better statistics. For each specimen, at least three scans were taken at different locations, to attain consistency in the concentration profiles.

3. Results and discussion

3.1. Evolution of the interfacial microstructures

It can be noted from the Cu–Ti binary phase diagram [19] shown in Fig. 1, that the maximum solubility of Cu in α-Ti is 1.6 at.% at 805 °C and that of Ti in Cu is 8 at.% at 885 °C. Seven stable compounds viz. $CuTi_3$, $CuTi_2$, CuTi, Cu_4Ti_3, Cu_3Ti_2, Cu_2Ti and Cu_4Ti are seen in the phase diagram. Out of which, only Cu_2Ti exists over a narrow temperature range of 870–890 °C.

Figure 2a, b and c show BSE micrographs of the couples annealed at 720 °C, 780 °C and 860 °C respectively, for 120 h each. The BSE micrographs of the diffusion zones of the Cu/Ti diffusion couples in Fig. 2a–c clearly show the formation of various intermetallic compounds in the form of layers, parallel to the original interface. The relative widths of these compounds are evident from the micrographs. Since the interfaces between the phases are wavy in nature, the widths of the layers were not constant throughout the diffusion zone. Therefore, the widths were measured at 5 different locations, and the average values were taken for further calculations.

The micrograph in Fig. 2a clearly shows that three distinct layers of intermediate compounds were formed at the interface. The widest layer (of about 25 μm) among the three, formed just adjacent to Ti, was identified as the CuTi phase. The next two layers on the Cu-side could be identified as Cu_4Ti_3 and Cu_4Ti and their widths were 5 μm and 16 μm respectively. The thicknesses of the layers of intermetallic compounds formed in the diffusion zone of the couples are listed in Table 1. A fourth compound of thickness ≈ 1–2 μm was observed to have formed at discrete locations along the CuTi/Ti interface. Micro-analysis of this phase at locations where the thickness was relatively large, using static beam condition in EPMA, revealed a composition close to $CuTi_2$. The BSE micrograph for the couple annealed at 780 °C (Fig. 2b) shows four layers of intermediate compounds and a solid solution phase adjacent to the Ti side. In addition to Cu_4Ti, CuTi and Cu_4Ti_3, a thin but continuous layer (about 1–2 μm) of $CuTi_2$ was found to form between CuTi and Ti. The thickness of these layers increased due to the increase in annealing temperature. Similar observations were reported in the related system of Cu–Zr [24, 25]. Bhanumurthy et al. [24] reported the formation of only two compounds, Cu_4Zr and $CuZr_2$, in the temperature range, 600–704 °C; whereas, Taguchi et al. [25] reported the formation of six intermediate compounds in the temperature range, 700–880 °C, of which the layer of $Cu_{10}Zr_7$ forms only above 855 °C with an incubation period.

Adjacent to the $CuTi_2$ phase, on the Ti side, a layer of β-Ti of about 8 μm was also identified (Fig. 2b). This solid solution layer showed a uniform composition of about 5–6 at.% Cu. The formation of such a β-Ti layer was attributed to the diffusion of Cu into Ti. Cu, being a β-stabilizer, diffuses into Ti and thereby stabilizes a layer of β-Ti. It is

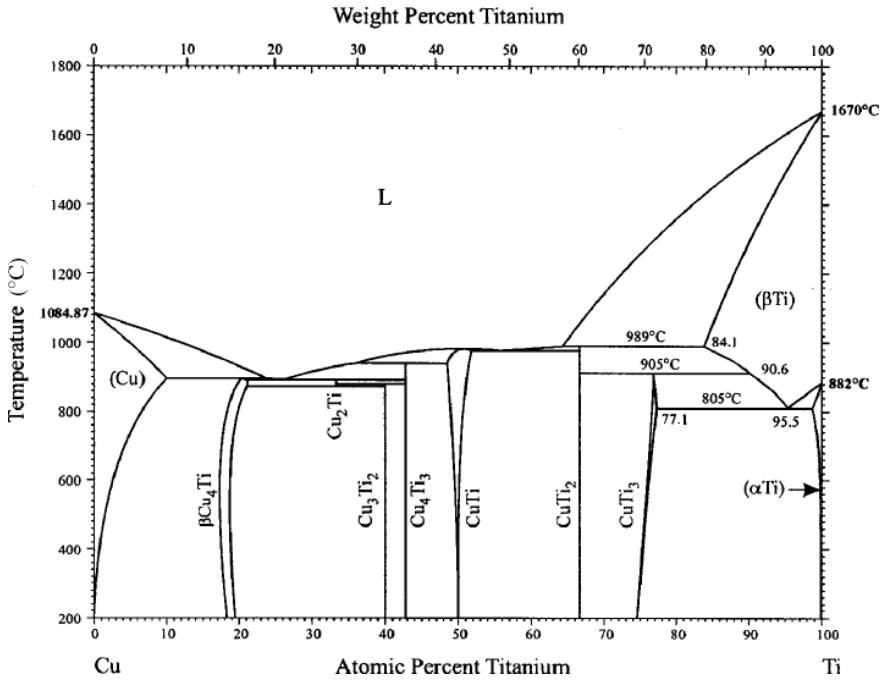

Fig. 1. Binary alloy phase diagram of the Cu–Ti system [19].

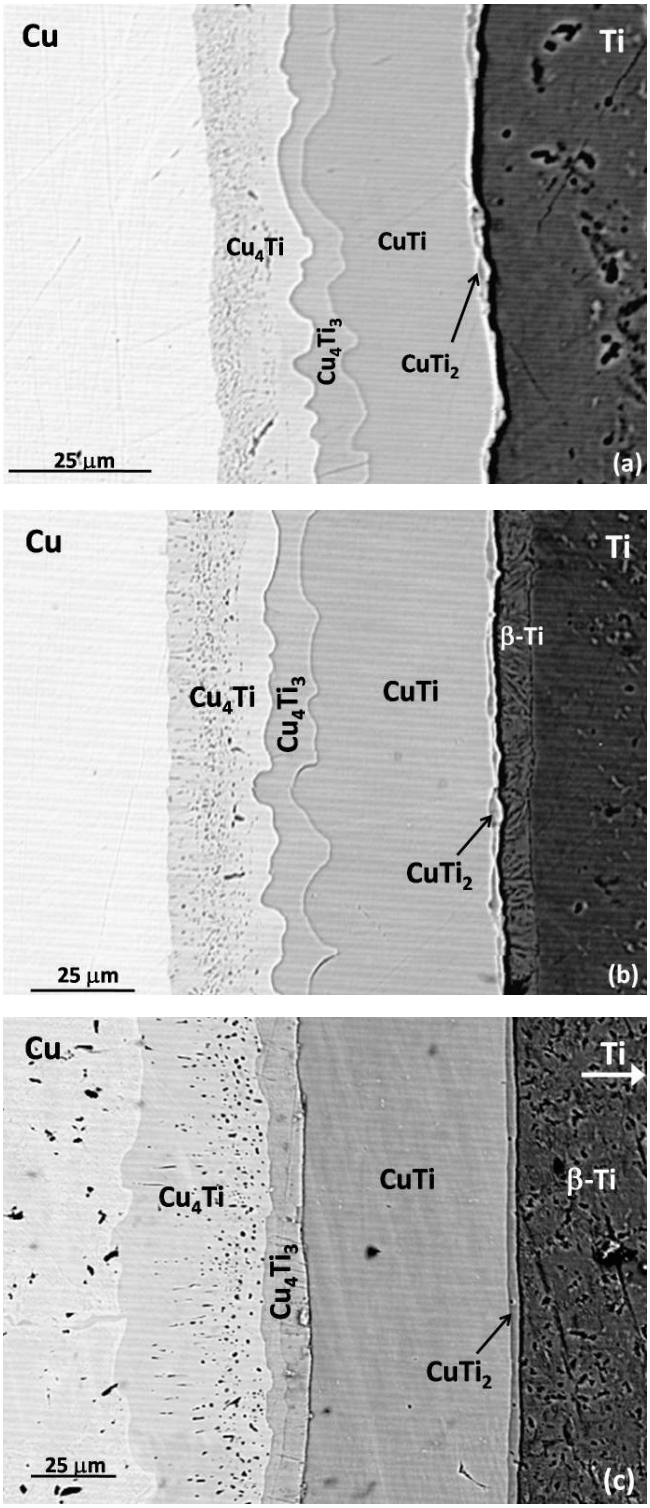

Fig. 2. Back-scattered electron micrographs of the diffusion zones of the Cu–Ti diffusion couples after annealing at (a) 720 °C, (b) 780 °C and (c) 860 °C for 120 h each. Different layers formed in the diffusion zone are labeled.

interesting to note that two different versions of the Cu–Ti phase diagram exist in literature, showing disagreement over the Ti rich part [19, 21]. The earlier version of the phase diagram [21] shows that the lowest temperature at which stable β-phase can exist is 790 °C, where the eutectoid reaction β-Ti ↔ α-Ti + $CuTi_2$ occurs. With the introduction of the $CuTi_3$ phase in the current version [19], the eutectoid temperature was modified to 805 °C, the associated reaction being β-Ti ↔ α-Ti + $CuTi_3$. It appears, therefore, that some amount of uncertainty exists regarding the eutectoid temperature. As the annealing temperature is very close to the eutectoid temperature, the local equilibrium at the interface may get altered due to the presence of interdiffusion flux of the Cu and Ti atoms across the diffusion zone. This might have led to the formation of the β-Ti layer. Such formation of β-solid solution phase is commonly observed in the diffusion couples of Ti- and Zr-based systems, especially those which undergo eutectoid transformations. For example, in the Ti-*X* and Zr-*X* systems (*X* = Cr, Cu, Ag, Au), the β-Ti and β-Zr solid solution phases appear in the diffusion zones and exhibit parabolic rate of growth [26]. As mentioned in Section 2.1, the thickness of the diffusion zone of the as-bonded diffusion couples was negligibly small (2–3 μm). Although the major portion of this diffusion zone is expected to be the CuTi phase [8, 12], a thin layer of β-Ti solid solution may also form. Subsequent furnace cooling could transform the β-Ti layer to α-Ti and a small fraction of $CuTi_3$. However, such small volume fraction of the $CuTi_3$ phase in the diffusion zone is not expected to have significant influence on the interdiffusion of Cu and Ti during the process of diffusion annealing.

Annealing at temperatures higher than 780 °C did not show the formation of any additional layer of intermetallic compound. Figure 2c shows a micrograph of the couple annealed at 860 °C, the highest temperature of annealing. As observed at 780 °C, this micrograph also shows the formation of Cu_4Ti, Cu_4Ti_3, CuTi and $CuTi_2$ intermetallic compounds. However, the layer of β-Ti was found to have grown to a large width of 500–520 μm at this temperature. Therefore, the entire layer could not be shown in Fig. 2c. The presence of Kirkendall pores could be observed in all the diffusion couples, close to copper, in the Cu_4Ti layer. Such an observation suggested a higher rate of diffusion of Cu due to lower melting point. Taguchi et al. [8] observed a slight movement of markers towards the Cu-rich side which also indicated a higher diffusion rate for Cu.

3.2. Concentration profiles

The concentrations obtained at different points were plotted against distance. Figure 3 shows typical concentration profiles for the diffusion zones of the couples annealed at 750 °C and 830 °C respectively. The steps in the profiles, where the composition remains fairly constant over a distance, correspond to the intermediate compounds formed in the diffusion zone. The three steps in Fig. 3a confirmed the formation of CuTi, Cu_4Ti_3 and Cu_4Ti. However, since the $CuTi_2$ phase does not form as a continuous layer at 750 °C, the step corresponding to it was not found in the concentration profile. The Cu_4Ti_3 phase showed negligible variation in composition within the layer, whereas, in the cases of CuTi and Cu_4Ti, the Ti-concentration varied within 1.3–2.8 at.% and 1.7–2.1 at.% respectively. This was in accordance with the solubility range of CuTi and Cu_4Ti, as shown in the Cu–Ti binary phase diagram (Fig. 1) [19]. The presence of a solubility range was utilized to determine the interdiffusion coefficients in these compounds, as described in Section 3.5.

The concentration profile for the couple annealed at 830 °C (Fig. 3b) showed the presence of four such steps cor-

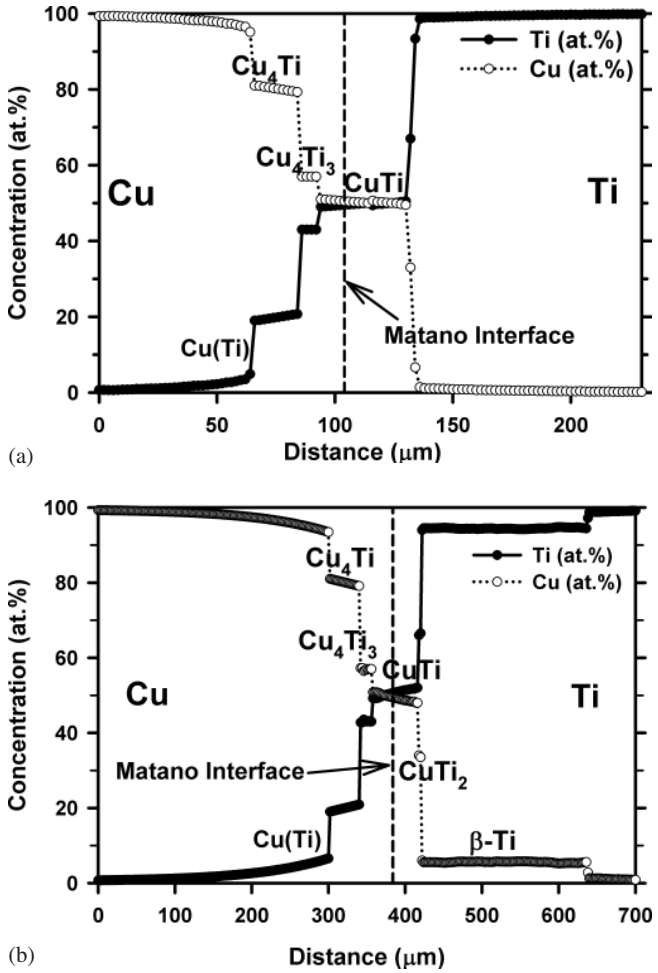

Fig. 3. Concentration profiles across the diffusion zone of the Cu–Ti diffusion couples annealed for 120 hours at (a) 750 °C and (b) 830 °C.

responding to Cu_4Ti, Cu_4Ti_3, CuTi and $CuTi_2$. The presence of a layer of β-Ti with a composition of 5.6 at.% Cu, was also found in the Ti-side of the diffusion zone. The concentration of Cu remained fairly constant throughout the layer, which indicated that the β-Ti phase did not undergo any solute partitioning during the process of quenching. This β-Ti layer was found to grow very fast with rise in temperature. The width of the layer was about 8 μm at 780 °C, 50 μm at 800 °C, 220 μm at 830 °C and at 860 °C it grew to as large as 500–520 μm. Such a rapid growth of the β-Ti layer may be attributed to higher rate of diffusion of Cu in Ti due to a corresponding rapid change in the solubility of Cu in β-Ti (Fig. 1) [19]. At 860 °C, i. e. the highest temperature of annealing, the solubility of Cu is as high as 10 at.%.

A continuous variation in the concentration of Ti in the region between Cu_4Ti and pure Cu was indicative of formation of Cu(Ti) terminal solid solution, as shown in Fig. 3a and b. The smooth transition of the concentration of Ti from 0 % to the solubility limit within the Cu(Ti) region, was utilised to determine the interdiffusion coefficient in this solid solution phase.

3.3. Sequence of phase formation

Out of the six stable intermediate compounds in the phase diagram, in the temperature range of study, only four (Cu_4Ti, Cu_4Ti_3, CuTi and $CuTi_2$) were formed at the diffusion zone. The phases $CuTi_3$ and Cu_3Ti_2, were not found to form in the diffusion zone within the resolution of the experimental techniques used in the present studies. In the course of a recent investigation on the chemical reactivity near 800 °C, Cu_3Ti_2 was found to be systematically absent in the reaction zone [27]. Andrieux et al. [28] showed, using isothermal diffusion experiments that the solid-state reaction for the formation of Cu_3Ti_2 is:

$$5\,Cu_4Ti_3 + Cu_4Ti \rightarrow 8\,Cu_3Ti_2 \qquad (1)$$

Being the last stage of a sequence of reactions, Cu_3Ti_2 has a long incubation time and proceeds at a very slow rate [28]. Such an absence of stable compounds in the diffusion zone, in comparison to the phase diagram, is often encountered and is reported in several systems. For example, Laik et al. [29] reported that, in the Zr–Al system, out of ten stable compounds present in the equilibrium phase diagram, only two formed in the diffusion zone. The absence of stable intermediate compounds in the diffusion zone has been a topic of extensive investigation [30, 31]. An excellent review by van Loo [30] deals with this in detail. Also, Dybkov [31] has cited more examples of such binary systems, including the present Cu–Ti system, which show the absence of stable intermediate compounds in the diffusion zone. The primary reasons for the absence of a stable compound in the diffusion zone are attributed to difficulty in its nucleation in the presence of the adjacent phases and a slow rate of diffusion within this phase, which is not sufficient to sustain its growth under such conditions.

The sequence of formation of the phases in the diffusion-zone during diffusion reaction is important in understanding the evolution of the microstructure. A number of models exist in the literature on prediction of the formation of the first phase [32–38]. Amongst these, the effective heat of formation (EHF) model proposed by Pretorius [36, 37] is the most recent and has successfully predicted the first phase of formation in many binary systems such as M–Al and M–Ge (M = metal). The EHF model combines the thermodynamic data with the concentrations of the reacting species at the growth interface. Based on this model, the EHF, $\Delta H'$, is defined as:

$$\Delta H' = \Delta H^0 \frac{C_e}{C_l} \qquad (2)$$

where, ΔH^0 is the standard heat of formation, C_e is the effective concentration of the limiting element at the interface, taken as the composition of the limiting element at the lowest liquidus temperature, and C_l is the concentration of the limiting element in the compound.

However, Pretorius' EHF model [36, 37] could not predict the first phase in some systems, where congruent and non-congruent compounds are simultaneously present. Bhanumurthy et al. [39] proposed a modification to the EHF model by incorporating a congruency factor, ΔH^f, and defined the modified effective heat of formation (MEHF) as:

$$\Delta H^m = \left(\Delta H^0 + \Delta H^f\right) \frac{C_e}{C_l} \qquad (3)$$

Here ΔH^f is assumed to be equal to the heat of crystallisation of the compound for congruent compounds and zero for non-congruent compounds formed at the interface. The

congruency factor can be empirically related to the melting point T_m of the intermediate phase by [39]:

$$\Delta H^f = 8.31\, T_m \text{ J mol}^{-1} \quad (4)$$

The MEHF model was successfully used to predict the first phase in various systems, for example, Pt – Si [39], Mn – Ge [39], Fe – Al [39] and Zr – Al [29]. On the basis of this model, the values of $\Delta H'$ and ΔH^m have been calculated for the compounds in the Cu – Ti system, relevant to the present study, using the ΔH^0 values reported by Hari Kumar et al. [40] and Colinet et al. [41]. These values are listed in Table 2. $CuTi_3$ is not included in the table due to non-availability of thermodynamic data. It can be seen that CuTi has the maximum negative values for both heat of formation (ΔH^0) as well as MEHF (ΔH^m) and hence, is expected to form first at the diffusion zone. As mentioned earlier, CuTi is the only congruent melting phase and is the widest of all the phases formed in the diffusion zone. Using first principle calculations, it was recently shown, that out of the seven stable and five metastable compounds in the Cu – Ti system, the most stable phase is CuTi [42]. Hence, it is expected to form first during the Cu – Ti diffusion reaction. Also, Liotard et al. [12] showed, using careful thin film experiments, that CuTi is the first phase to form by diffusion reaction.

Once the CuTi phase forms at the Cu/Ti interface, appearance of additional layers between Cu and CuTi is decided by the prevailing thermodynamic and kinetic conditions at the Cu/CuTi interface. Since the experimental results show formation of Cu_4Ti and Cu_4Ti_3 phase layers between the Cu(Ti) terminal solid solution and CuTi, the driving forces required for their formation were evaluated, assuming a local thermodynamic equilibrium at the Cu(Ti)/CuTi interface.

A terminal solid solution phase (Φ) can be described as a single sub-lattice model, where the molar free-energy of the phase is expressed by the relationship [43]:

$$G_m^\Phi = \sum_{i=\text{Cu,Ti}} x_i^\Phi\, {}^0G_i^\Phi + RT \sum_{i=\text{Cu,Ti}} x_i^\Phi \ln x_i^\Phi + x_{Cu}^\Phi\, x_{Ti}^\Phi\, L_{Cu,Ti}^\Phi \quad (5)$$

where, ${}^0G_i^\Phi$ and x_i^Φ are the molar free energy of component i and the mole fraction of i in the phase Φ, respectively. The last term of the expression represents the excess free energy and its composition dependence is given by a Redlich – Kister polynomial [44]:

$$x_{Cu}^\Phi\, x_{Ti}^\Phi\, L_{Cu,Ti}^\Phi = x_{Cu}^\Phi\, x_{Ti}^\Phi \sum_{\nu=0}^{n} {}^\nu L_{Cu,Ti}^\Phi \left(x_{Cu}^\Phi + x_{Ti}^\Phi\right)^\nu \quad (6)$$

The free energy of the Cu(Ti) terminal solid solution (Φ = fcc-A1) was modelled assuming a regular solution behaviour (ν = 1). The intermediate phases Cu_4Ti, Cu_4Ti_3 and CuTi were modelled as stoichiometric line compounds ($\theta = Cu_pTi_q$). The Gibbs free energy per mole of formula unit of such a compound is given by [40]:

$$G^\theta = (p+q)(a^\theta + b^\theta T) \quad (7)$$

The values of the thermodynamic parameters, a^θ, b^θ and ${}^\nu L_{Cu,Ti}^\Phi$ used in the present calculations were optimised by Hari Kumar et al. [40] for the Cu – Ti system. Standard Elemental References (SER) were taken as the reference state and the STGE data for pure elements [45] were used for the calculations.

The driving force for formation of a compound at the Cu(Ti)/CuTi interface is determined by the decrease in free energy of the system due to its formation. The driving forces for formation of Cu_4Ti, Cu_4Ti_3 were found to be close to each other, $\Delta G_{Cu_4Ti} \approx 510$ J mol^{-1} and $\Delta G_{Cu_4Ti_3} \approx 540$ J mol^{-1}, which implied almost equal thermodynamic probability of formation for both. However, as discussed in a later section, the interdiffusion coefficients of CuTi is almost an order of magnitude higher than that of the Cu(Ti) solid solution. Such a condition may lead to a rapid buildup of the concentration of Ti in Cu(Ti), at the vicinity of the Cu(Ti)/CuTi interface; possibly resulting in nucleation of the Cu_4Ti phase, since the solubility of Ti in Cu(Ti) is limited to 8 at.% [21]. Subsequently, the formation of a layer of Cu_4Ti_3 at the Cu_4Ti/CuTi interface, may be due to a solid state reaction of the type:

$$Cu_4Ti + 8\,CuTi \rightarrow 3\,Cu_4T_3 \quad (8)$$

Such a scheme of reaction would necessitate an incubation period for the formation of Cu_4Ti and Cu_4Ti_3. The work by Liotard et al. [12] on solid-state reaction of Cu – Ti thin film provided experimental evidence for the existence of such an incubation period. It was shown that the second phase in the diffusion zone (metastable Cu_3Ti phase), formed after 4 hrs of heat treatment at 400 °C [12]. Similarly, Andrieux et al. [28] showed that though Cu_4Ti formed after 11.5 min, Cu_4Ti_3 appeared only after 30 min of heating of Ag – Cu – Ti powder compacts at 790 °C.

Table 2. The values of heat of formation (ΔH^0), effective heat of formation ($\Delta H'$) and modified heat of formation (ΔH^m), for the various intermediate phases in the Cu–Ti system.

Phase	Composition (at.% Cu)	Congruency	Limiting element	ΔH^0 [Ref.]	$\Delta H'$	ΔH^m
				(kJ(mol of atom)$^{-1}$)		
Cu_4Ti	80.00	NC	Cu	–5.53 ± 1.07 [41]	–5.05	–5.05
Cu_2Ti	66.67	NC	Cu	–5.88 [40]	–6.53	–6.53
Cu_3Ti_2	60.00	NC	Cu	–9.36 ± 0.6 [41]	–11.39	–11.39
Cu_4Ti_3	57.14	NC	Cu	–9.65 ± 0.88 [41]	–12.33	–12.33
CuTi	50.00	C	Cu	–11.12 ± 1.72 [41]	–16.24	–31.51
$CuTi_2$	33.33	NC	Cu	–8.20 ± 1.62 [41]	–17.96	–17.96

C = Congruent, NC = Non-congruent

The formation of $CuTi_2$ phase in discrete regions along the CuTi/Ti interface at lower temperatures, 750 and 780 °C, is indicative of late nucleation of this compound in the diffusion zone. Therefore, the sequence of phase formation may be described as: CuTi → Cu_4Ti → Cu_4Ti_3 → $CuTi_2$.

3.4. Kinetics of phase growth

The growth of the intermediate phases formed in the Cu–Ti system was reported to be diffusion controlled and hence follows a parabolic relationship of the type [8, 12]:

$$w^2 = Kt \tag{9}$$

where w is the width of the phase layer, K is the parabolic coefficient and t is the time of annealing. The values of the parabolic coefficient (K) for each of the compounds were plotted against $1/T$ and fitted to straight lines in Fig. 4. The data points for each compound were fitted to straight lines using linear regression. Such linear fit in the ln K versus $1/T$ plot suggested that the growth of the compounds is a thermally activated process. The coefficient K follows an Arrhenius type of temperature dependence:

$$K = K_0 \exp(-Q_K/RT) \tag{10}$$

where, K_0 is the pre-exponential factor, Q_K is the activation energy for growth, R is the universal gas constant and T is the temperature in absolute scale. The values of Q_K and K_0 can be determined from the values of the slopes and intercepts of the straight lines fitted in Fig. 4 and tabulated in Table 3.

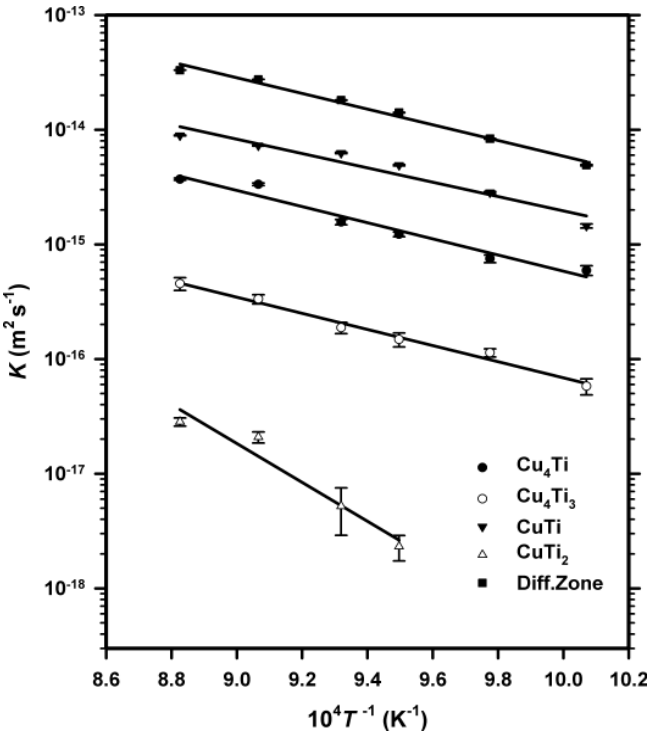

Fig. 4. Temperature dependence of parabolic coefficient (K) of the layers of compounds Cu_4Ti, Cu_4Ti_3, CuTi, $CuTi_2$ and the entire diffusion zone formed in the diffusion zone.

The activation energies required for the growth of the various layers are as follows: $Q_K^{Cu_4Ti} = 134.7 \pm 2.5$ kJ mol^{-1} for Cu_4Ti, $Q_K^{Cu_4Ti_3} = 134.5 \pm 2.3$ kJ mol^{-1} for Cu_4Ti_3, $Q_K^{CuTi} = 119.8 \pm 2.9$ kJ mol^{-1} for CuTi and $Q_K^{DZ} = 131.0 \pm 1.1$ kJ mol^{-1} for the entire diffusion zone. The uncertainty in the activation energy values originates from the uncertainty in the values of the slope of linear regression lines. It may be mentioned here that since the thickness of the $CuTi_2$ layer is very small (1–4 μm), the error involved in its measurement is very high. This leads to a large amount of uncertainty in the values of the activation energy for this layer. Therefore, the calculation of the activation energy for $CuTi_2$ was not attempted and hence not included in Table 3.

The activation energy values of the intermetallic compound layers are compared with those reported in the literature [8, 11, 12]. Taguchi et al. [8] evaluated the activation energies for the growth of Cu_4Ti_3 and CuTi as $Q_K^{Cu_4Ti_3} = 104$ kJ mol^{-1} and $Q_K^{CuTi} = 125$ kJ mol^{-1} respectively. Although the value of Q_K^{CuTi} is comparable to the present values, that of $Q_K^{Cu_4Ti_3}$ is lower than those. The values of Q_K, calculated using bulk diffusion couples in the present study, were substantially lower in comparison to that of the phases, Cu_3Ti and CuTi formed in thin film experiments in the temperature range 350–450 °C ($Q_K^{Cu_3Ti} = 175.6$ kJ mol^{-1} and $Q_K^{CuTi} = 142.8$ kJ mol^{-1} [12]) and 400–600 °C ($Q_K^{Cu_3Ti} = 171.8$ kJ mol^{-1} and $Q_K^{CuTi} = 155.4$ kJ mol^{-1} [11]). However, the values of K_0 for CuTi and Cu_4Ti_3 (Table 3) are comparable with those reported by Taguchi et al. [8] ($K_0^{CuTi} = 5.3 \times 10^{-9}$ m^2 s^{-1} and $K_0^{Cu_4Ti_3} = 1.3 \times 10^{-11}$ m^2 s^{-1}).

3.5. Diffusion coefficient of compounds formed in the diffusion zone

The concentration-dependent interdiffusion coefficient ($\tilde{D}$) of a binary system is generally evaluated using the Boltzmann–Matano (B–M) method [46, 47] using the concentration profile across the diffusion zone. The value of $\tilde{D}$ at any concentration C^* can be determined using the relationship:

$$\tilde{D}(C^*) = -\frac{1}{2t}\left(\frac{dx}{dC}\right)_{C=C^*} \int_{C^{-\infty}}^{C^*} (x - x_0)\, dC \tag{11}$$

where t is the time of annealing, $\left(\frac{dx}{dC}\right)_{C=C^*}$ is the inverse of the concentration gradient at concentration C^*; $C^{-\infty}$ is the concentration at the extreme left end and x_0 is the position of the Matano interface (MI). Equation (11) can be applied to both single-phase and multi-phase diffusion couples. However, in the case of multi-phase diffusion couples, the concentration gradient inverse $\left(\frac{dx}{dC}\right)$ can be approximated

Table 3. The values of the activation energy (Q_K) and pre-exponential factor (K_0) for the growth of the compounds formed in the diffusion zone.

Parameter	Cu_4Ti	Cu_4Ti_3	CuTi	Diffusion zone
Q_K (kJ mol^{-1})	134.7 ± 2.5	134.5 ± 2.3	119.8 ± 2.9	131.0 ± 1.1
K_0 (× 10^{-9} m^2 s^{-1})	$6.37^{+4.32}_{-3.25}$	$0.73^{+0.37}_{-0.21}$	$3.55^{+2.48}_{-2.06}$	$41.02^{+26.94}_{-19.21}$

to $\left(\frac{\Delta x}{\Delta C}\right)$ within an intermediate phase, assuming linear variation of concentration with distance. The composition C^* is approximated to the average concentration of the compound, denoted as $C_{1/2}$. Therefore, in such cases, Eq. (11) can be rewritten as

$$\tilde{D} = -\frac{1}{2t}\left(\frac{\Delta x}{\Delta C}\right)\int_{C^{-\infty}}^{C_{1/2}} (x - x_0)\,\mathrm{d}C \qquad (12)$$

This method is more popularly known as the Boltzmann–Matano–Heumann (B–M–H) method [48].

Since the change in total volume of the diffusion couple upon interdiffusion influences the estimation of the diffusion coefficients, correction related to the variation in molar volume becomes necessary when the change in volume is large [49]. Based on the crystallographic data available [50], the molar volume of the compounds and the β-Ti phase formed were calculated. An estimation of the total change in volume in the diffusion couples showed that it varied within 3–3.5 % for all the diffusion couples. Moreover, the lattice parameter of dilute Cu–Ti alloys is known to be independent of the composition [51]. Therefore, correction for such negligible change in volume was not deemed necessary.

It may be noted that for an intermediate phase with a negligible homogeneity range, $\Delta C \approx 0$, the interdiffusion coefficient cannot be evaluated using Eq. (12). However, an integrated diffusion coefficient [52, 53] can instead be calculated over a concentration range (ΔC) by integrating the interdiffusion flux $\tilde{J}$ over the thickness of the compound layer [$w = (x_2 - x_1)$].

$$\tilde{D}^{\mathrm{int}} = \int_{x_1}^{x_2} \tilde{J}\mathrm{d}x = \tilde{D}\Delta C \qquad (13)$$

Out of the four intermediate compounds formed in the diffusion zones of the Cu–Ti diffusion couples, only two of them, Cu_4Ti and CuTi are non-stoichiometric and hence have solubility range. While Cu_4Ti has a solubility range of 19.1 to 22 at.% Ti [21, 54, 55], CuTi exists between 48 to 52 at.% Ti [21, 56]. The interdiffusion coefficients of these phases, $\tilde{D}_{\mathrm{CuTi}}$ and $\tilde{D}_{\mathrm{Cu_4Ti}}$, were evaluated using the B–M–H method (Eq. (12)) [48] for each temperature of annealing. The integrated diffusion coefficient in the phase Cu_4Ti_3 ($\tilde{D}^{\mathrm{int}}_{\mathrm{Cu_4Ti_3}}$) was evaluated using Eq. (13), since it is a line compound [19, 21]. Table 4 shows the values of $\tilde{D}_{\mathrm{CuTi}}$, $\tilde{D}_{\mathrm{Cu_4Ti}}$ and $\tilde{D}^{\mathrm{int}}_{\mathrm{Cu_4Ti_3}}$ and the variation in the range of concentration of Ti in these layers, ΔC_{CuTi} and $\Delta C_{\mathrm{Cu_4Ti}}$.

In order to determine the temperature dependence, the values of $\tilde{D}_{\mathrm{CuTi}}$, $\tilde{D}_{\mathrm{Cu_4Ti}}$ and $\tilde{D}^{\mathrm{int}}_{\mathrm{Cu_4Ti_3}}$ were plotted against temperature inverse ($1/T$) in a semi-log plot as shown in Fig. 5. The data points for each of these parameters were fitted to an Arrhenius relation using linear regression:

$$\tilde{D} = \tilde{D}_0 \exp\left(\frac{-Q}{RT}\right) \qquad (14)$$

The activation energy (Q) and the pre-exponential factor (D_0) for interdiffusion in the phases Cu_4Ti, CuTi and Cu_4Ti_3 were evaluated from the slope and intercept values of the plots. The temperature dependence of $\tilde{D}_{\mathrm{CuTi}}$, $\tilde{D}_{\mathrm{Cu_4Ti}}$and $\tilde{D}^{\mathrm{int}}_{\mathrm{Cu_4Ti_3}}$ is expressed as

$$\tilde{D}_{\mathrm{CuTi}} = \left(1.79^{+1.26}_{-0.74}\right) \times 10^{-4} \exp\left(\frac{-187.7 \pm 3.2\ \mathrm{kJ\ mol^{-1}}}{RT}\right) \mathrm{m^2\ s^{-1}} \qquad (15a)$$

$$\tilde{D}_{\mathrm{Cu_4Ti}} = \left(5.97^{+4.30}_{-2.49}\right) \times 10^{-5} \exp\left(\frac{-192.2 \pm 3.4\ \mathrm{kJ\ mol^{-1}}}{RT}\right) \mathrm{m^2\ s^{-1}} \qquad (15b)$$

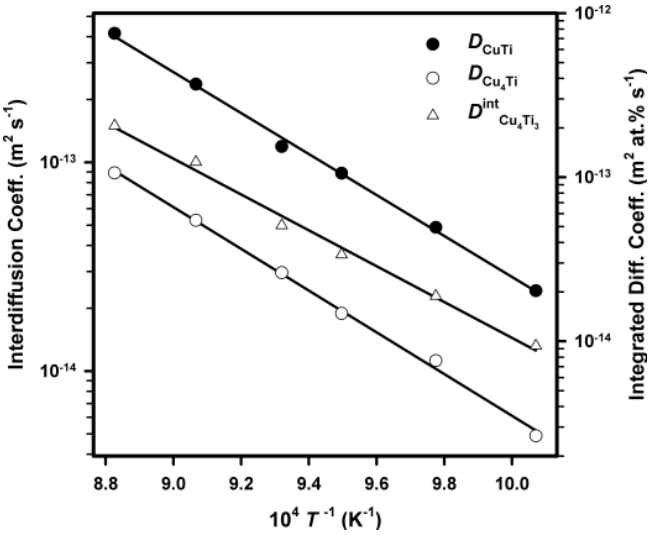

Fig. 5. Temperature dependence of interdiffusion coefficients of CuTi and Cu_4Ti ($\tilde{D}_{\mathrm{CuTi}}$ and $\tilde{D}_{\mathrm{Cu_4Ti}}$) and integrated diffusion coefficient of Cu_4Ti_3 ($\tilde{D}^{\mathrm{int}}_{\mathrm{Cu_4Ti_3}}$).

Table 4. Interdiffusion coefficients ($\tilde{D}_{\mathrm{CuTi}}$ and $\tilde{D}_{\mathrm{Cu_4Ti}}$), range of concentration of Ti (ΔC_{CuTi} and $\Delta C_{\mathrm{Cu_4Ti}}$) in the layers of CuTi and Cu_4Ti and the integrated diffusion coefficient ($\tilde{D}^{\mathrm{int}}_{\mathrm{Cu_4Ti_3}}$) in Cu_4Ti_3, at different temperatures.

Temperature (°C)	CuTi		Cu_4Ti		Cu_4Ti_3
	$\tilde{D}_{\mathrm{CuTi}}$ ($\times 10^{-14}$ m^2 s^{-1})	$\tilde{D}_{\mathrm{CuTi}}$ (at.%)	$\tilde{D}_{\mathrm{Cu_4Ti}}$ ($\times 10^{-14}$ m^2 s^{-1})	$\Delta C_{\mathrm{Cu_4Ti}}$ (at.%)	$\tilde{D}^{\mathrm{int}}_{\mathrm{Cu_4Ti_3}}$ ($\times 10^{-14}$ m^2 at.% s^{-1})
720	2.43	1.3	0.488	1.7	0.938
750	4.89	1.5	1.12	1.7	1.89
780	8.87	1.7	1.89	1.7	3.37
800	11.89	2.0	2.96	1.8	5.08
830	23.70	2.6	5.28	1.9	12.38
860	41.52	2.8	8.90	2.1	20.62

$$\tilde{D}^{\text{int}}_{Cu_4Ti_3} = \left(8.94\ ^{+7.67}_{-4.12}\right) \times 10^{-4} \exp\left(\frac{-209.2 \pm 4.3\ \text{kJ mol}^{-1}}{RT}\right) \text{m}^2\ \text{at.\%}\ \text{s}^{-1} \quad (15c)$$

The values for the diffusion parameters, Q and D_0, for the compounds CuTi, Cu_4Ti and Cu_4Ti_3 are $Q^{CuTi} = 187.7 \pm 3.2$ kJ mol^{-1}, $D_0^{CuTi} = 1.79^{+1.26}_{-0.74} \times 10^{-4}$ m^2 s^{-1}, $Q^{Cu_4Ti} = 192.2 \pm 3.4$ kJ mol^{-1}, $D_0^{Cu_4Ti} = 5.97^{+4.30}_{-2.49} \times 10^{-5}$ m^2 s^{-1}, $Q^{Cu_4Ti_3} = 209.2 \pm 4.3$ kJ mol^{-1} and $D_0^{Cu_4Ti_3} = 8.94^{+7.67}_{-4.12} \times 10^{-4}$ m^2 at.% s^{-1}.

Taguchi et al. [8] estimated the values of interdiffusion coefficients ($\tilde{D}$) for CuTi and Cu_4Ti_3, using a constant value of solubility range $\Delta C = 1$ at.% for both the compounds, at all temperatures. Since the value of ΔC was found to change by a factor of 2 for CuTi within this temperature range (Table 4), such an assumption may lead to erroneous results. Further, thermodynamic evaluation of the Cu_4Ti_3 compound showed it to be a stoichiometric line compound without any solubility range, i.e., $\Delta C \approx 0$ [19, 21]. As discussed earlier, in such a situation the evaluation of interdiffusion coefficient $\tilde{D}_{Cu_4Ti_3}$ is not justified. The diffusion parameters of Cu_4Ti_3 determined by using the integrated diffusion coefficient in the present study, therefore, seem to be more realistic. The earlier reported values of diffusion parameters of CuTi, $Q^{CuTi} = 183$ kJ mol^{-1} and $D_0^{CuTi} = 1.1 \times 10^{-4}$ m^2 s^{-1} [8], are comparable with the present values.

3.6. Interdiffusion coefficient in the Cu(Ti) solid solution

Concentration dependent interdiffusion coefficients ($\tilde{D}$) in solid solutions are usually determined by using Boltzmann–Matano [46, 47] and Sauer–Freise [57] methods. However, both these methods attempt to solve Fick's law numerically and involve estimation of slopes and areas of the concentration profiles. A serious disadvantage of using such a method is that it incorporates a considerable amount of uncertainty in the values of the slope and area at the ends of the concentration range, which leads to erroneous diffusion coefficient values [58, 59]. On the other hand, estimation of impurity diffusion coefficients and determination of the mechanism of diffusion warrants evaluation of interdiffusion coefficient at low concentrations with sufficient accuracy. In order to circumvent this problem, Hall's analytical solution [58] was used to determine the values of $\tilde{D}$ in the Cu(Ti) solid solution at different concentration values. The relation for $\tilde{D}$ at concentration C^* can be expressed as

$$\tilde{D}(C^*) = \frac{1}{4h^2} + \frac{k\sqrt{\pi}}{4h^2} \exp(u^2)\,[1 + \text{erf}(u)] \quad (16)$$

The variable u is defined as

$$\frac{C}{C_0} = \frac{1 + \text{erf}(u)}{2} \quad (17)$$

where C_0 is the concentration range ($C^{+\infty} - C^{-\infty}$) and erf($u$) is the error function of u. Here, the variables C and x are alternatively expressed in terms of u and the Boltzmann parameter, $\lambda (= x\sqrt{t})$ respectively and thus, the concentration profile is transformed to a plot of u against λ. The nature of variation of such plot can be expressed by a linear relationship, $u = h\lambda + k$ [58]. The values of parameters h and k are determined from the slope and intercept of the straight line fitted to the data points of the $u-\lambda$ plot.

The interdiffusion coefficients ($\tilde{D}$) in the Cu(Ti) solid solution were evaluated in the entire concentration range, $C_{Ti} \leq 5.0$ at.%, at intervals of 0.5 at.%, for all the temperatures. As shown in Fig. 6, the logarithm of $\tilde{D}$ was found to decrease linearly with increase in Ti concentration (C_{Ti}) in this concentration range. The data points for each of these temperatures were fitted to straight lines using linear regression and were extrapolated to infinite dilution ($C_{Ti} \approx 0$), to determine the impurity diffusion coefficient of Ti in Cu matrix.

The temperature dependence of $\tilde{D}$ at different compositions (Cu 0.5–4.0 at.% Ti) was determined by an Arrhenius-plot as shown in Fig. 7. The activation energies (Q) and pre-exponential factors (D_0) were evaluated for these compositions in the Cu(Ti) solid solution, using the Arrhenius relation (Eq. 14). Figure 8 shows that both the parameters Q and logD_0 increase linearly with the Ti-concentration

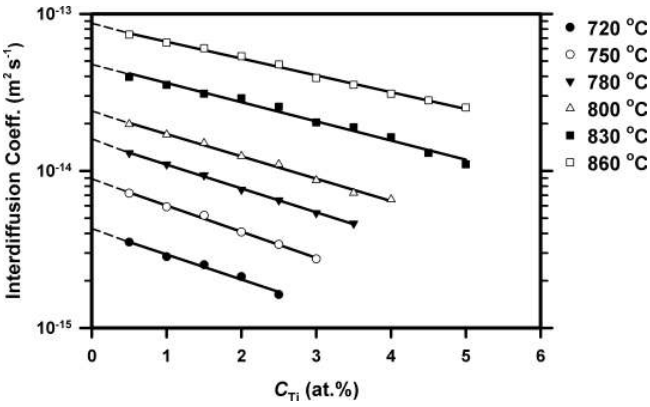

Fig. 6. Variation in the interdiffusion coefficient ($\tilde{D}$) in the Cu(Ti) solid solution as a function of concentration of Ti (C_{Ti}). The impurity diffusivity of Ti in pure Cu (D_{Ti}^{Cu}) is evaluated by extrapolating $\tilde{D}$ to Cu-0 % Ti.

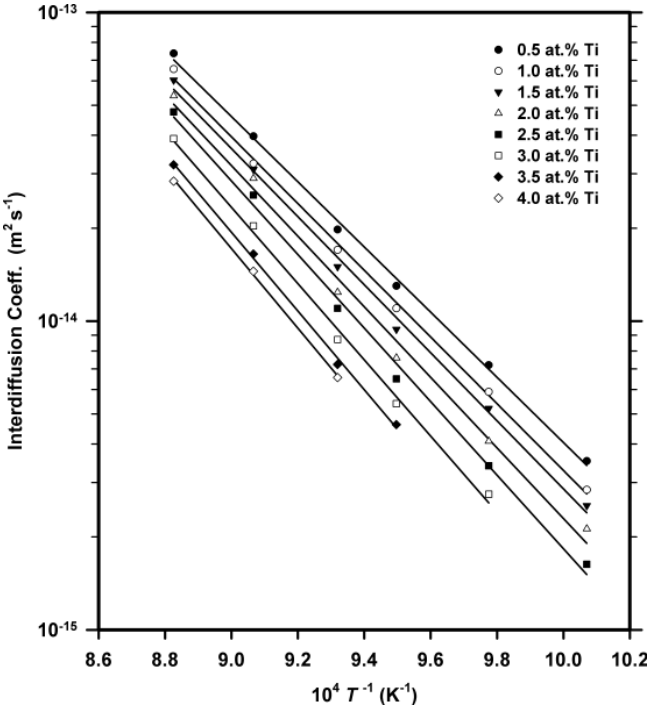

Fig. 7. Temperature dependence of the interdiffusion coefficient ($\tilde{D}$) in the Cu(Ti) terminal solid solution.

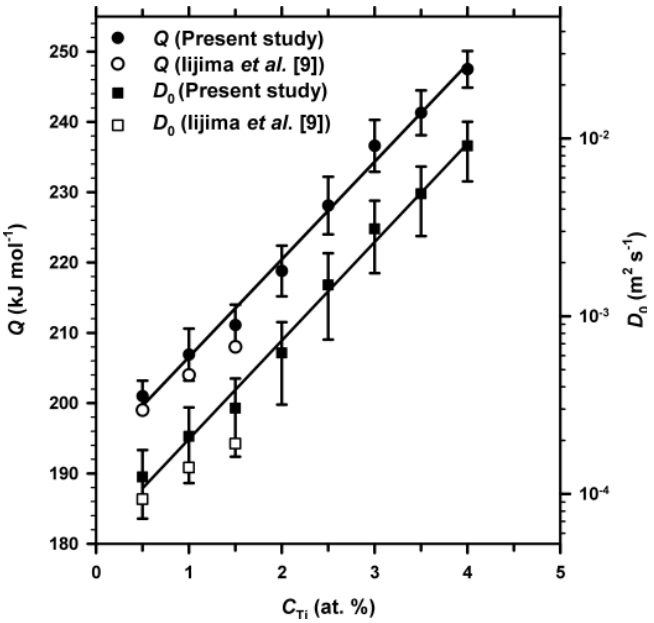

Fig. 8. Plot showing the linear variation of the activation energy (Q) and the pre-exponential factor (D_0) for interdiffusion in the Cu(Ti) solid solution with concentration of Ti (C_{Ti}). The present values are compared with results of Iijima et al. [9].

(C_{Ti}). The composition dependence of Q and $\log D_0$, evaluated from Fig. 8 for the range $0.5 \leq C_{Ti} \leq 4.0$ at.%, can be expressed as:

$$\log D_0(\mathrm{m^2\ s^{-1}}) = (-4.30 \pm 0.064) + (0.572 \pm 0.024)\, C_{Ti}(\mathrm{at.\%}) \qquad (18a)$$

$$Q(\mathrm{kJ\,mol^{-1}}) = (191.5 \pm 1.7) + (14.29 \pm 0.62) C_{Ti}(\mathrm{at.\%}) \qquad (18b)$$

It was shown by Nagarjuna et al. [60] that Ti has a pronounced effect of solid solution strengthening in Cu, due to large atomic size misfit. They also reported a significant increase in the electrical resistivity of copper by addition of Ti. It may be assumed that such effects might be responsible for the decrease in the interdiffusion coefficient ($\tilde{D}$) with increase in the Ti concentration in the Cu(Ti) solid solution, as observed in Fig. 6. This further explains the increase in the values of D_0 and Q with the increase in the Ti content (Fig. 8 and Eq. (18)).

Iijima et al. [9] evaluated the values of the parameters $\tilde{D}$, Q and D_0 for the Cu(Ti) solid solution following the B–M method [46, 47], but limited to the concentration range, $C_{Ti} \leq 1.5$ at.% Ti. These values were found to be systematically lower in comparison to the present values (Fig. 8), possibly due to inherent deficiency of B–M method in determining values of $\tilde{D}$ at low concentrations [59]. It is interesting to note that activation energy for precipitation and coarsening of β-Cu_4Ti phase (207 kJ mol^{-1}) from super-saturated Cu(Ti) solid solution [5] is in good agreement with the activation energy for interdiffusion in the Cu(Ti) solid solution. This confirms that the coarsening process of such precipitates occurs by diffusion-controlled growth mechanism.

3.7. Impurity diffusion coefficient of Ti in Cu

The impurity diffusion coefficients of Ti in pure Cu (D_{Ti}^{Cu}) were determined by extrapolation of the straight lines in Fig. 6 to infinite dilution $C_{Ti} \to 0$, i.e., at Cu-0% Ti. The values of D_{Ti}^{Cu} at different temperatures are tabulated in Table 5. The temperature dependence of D_{Ti}^{Cu} was determined by plotting the same against temperature inverse on a semi-log plot, as shown in Fig. 9. A linear regression fitting of the data points of the plot indicated an Arrhenius-type of temperature dependence of D_{Ti}^{Cu} (Eq. (14)). The activation energy (Q^{Ti}) and pre-exponential factor (D_0^{Ti}) were determined from the slope and intercept values of the plot. The temperature dependence of D_{Ti}^{Cu} along with the probable errors is expressed by the following equation:

$$D_{Ti}^{Cu} = \left(9.92^{+0.74}_{-0.42}\right) \times 10^{-5} \exp\left(\frac{-200.2 \pm 3.4\ \mathrm{kJ\,mol^{-1}}}{RT}\right) \mathrm{m^2\ s^{-1}} \qquad (19)$$

The earlier reported values of D_{Ti}^{Cu} [9], estimated using the Boltzmann–Matano method, were lower than those determined in the present study (Fig. 9). However, the values of the parameters, Q^{Ti} (= 196 kJ mol^{-1}) and D_0^{Ti} (= 6.9×10^{-5} m^2 s^{-1}) [9], were comparable with the present values. The values of impurity diffusion parameters, when compared with those of self-diffusion of copper (D_{Cu}^{Cu}), Q^{Cu} = 211 kJ mol^{-1} and $D_0^{Cu} = 7.8 \times 10^{-5}$ m^2 s^{-1} [61], the difference between the activation energies for impurity and self diffusion, ΔQ (Q^{Ti}

Table 5. Impurity diffusivity of Ti in pure Cu (D_{Ti}^{Cu}) at different temperatures.

Temperature (°C)	D_{Ti}^{Cu} ($\times 10^{-15}$ m^2 s^{-1})
720	4.3
750	8.9
780	16.8
800	24.1
830	47.8
860	87.2

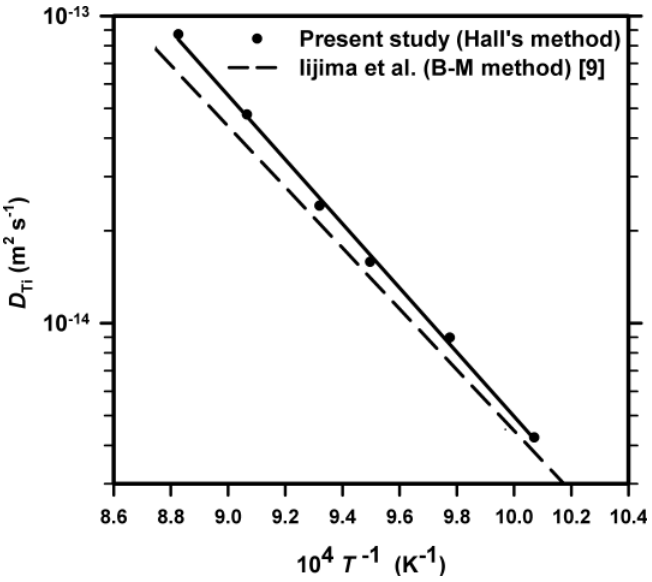

Fig. 9. Temperature dependence of the impurity diffusivity of Ti in pure Cu (D_{Ti}^{Cu}). The present values, determined using Hall's method, are compared with results of Iijima et al. [9], determined using Boltzmann–Matano (B–M) method.

$-Q^{Cu}$) was found to be -10.8 kJ mol^{-1}. Such negative values of ΔQ suggest high binding energy for impurity–vacancy pairs, according to the theory of vacancy diffusion [62, 63].

The impurity diffusion parameters, Q^{Ti} and D_0^{Ti}, of Ti were compared with those of other Cu-X systems (X = Ru, V, Mn, Cd, Pb, Tl, Sn, Rh, Ni, W, Pd, Fe, Ag, Ga, Ge, Hg, As, Zn, Au, Cr and Nb) [61, 64]. Several empirical correlations between the pre-exponential factor, D_0, and the activation energy, Q, for impurity diffusion in metals are available in literature [65–67]. Swalin [66] derived an equation based on the Lazarus theory [68] to correlate Q and D_0. According to Swalin [66], the slope of the plot of log D_0 and Q for different impurity elements in a particular solvent, (d log D_0/dQ), should remain constant.

The values of logD_0 and Q for impurity diffusion of various elements in Cu are plotted in Fig. 10. The data points in this plot were fitted to straight line using linear regression. The plot also shows the band for 99 % confidence level. The values for Ti obtained from the present analysis fitted close to the straight line within this band. The value of the slope of the straight line (d log D_0/dQ = 1.32×10^{-5} mol J^{-1}) is comparable with the values reported by Pelleg [69] (6.3×10^{-5} mol J^{-1}) for Cu. The value of the slope seems to be more refined, as the number of data points are large in number as compared to the earlier report [69]. Later on, Beke et al. [67] proposed a general expression for impurity diffusion. They showed that in a plot of $\ln(D_0^{imp}/D_0^{self})$ versus $\Delta Q/T_m$, the data points for various impurity elements should fall in a straight line. Such a plot for impurity diffusion in Cu matrix is shown in Fig. 10. Here, D_0^{imp} is the pre-exponential factor for diffusion of the impurity atom and D_0^{self} is the pre-exponential factor for the self diffusion in the matrix (Cu in the present case). ΔQ (= $Q^{imp} - Q^{self}$) is the difference between the activation energies and T_m is the melting point of the matrix. The slope of the straight line, fitted using least square method, was 4.16×10^{-2} mol K J^{-1}, which is in good agreement with similar value reported earlier ($(4.3 \pm 0.9) \times 10^{-2}$ mol K J^{-1} by Beke et al. [67]). The impurity diffusion coefficient value of Ti in Cu evaluated in the present study is therefore consistent with the related theories suggested by Swalin [66] and Beke [67].

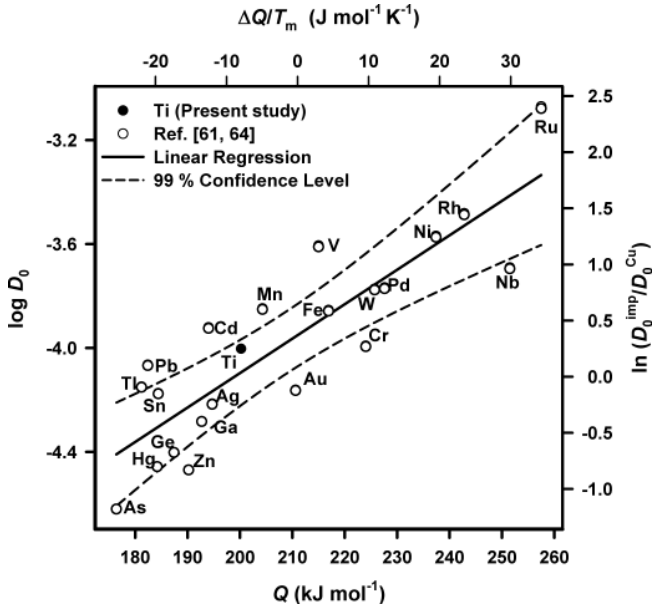

Fig. 10. Variation of the pre-exponential factor (D_0) with activation energy (Q) and ln (D_0^{imp}/D_0^{Cu}) with $\Delta Q/T_m$ for impurity diffusion in Cu.

4. Conclusions

Diffusion reaction between Cu and Ti in the temperature range of 720–860 °C, using bulk diffusion couples, resulted in the formation of four layers of intermediate compounds in the diffusion zone, viz., Cu_4Ti, Cu_4Ti_3, CuTi and $CuTi_2$. The values for activation energies for the growth of these compounds were found to be $Q_K^{Cu_4Ti}$ = 134.7 kJ mol^{-1}, $Q_K^{Cu_4Ti_3}$ = 134.5 kJ mol^{-1}, Q_K^{CuTi} = 119.8 kJ mol^{-1}. A layer of β-Ti formed on the Ti side of the diffusion zone at and above 780 °C, due to stabilization of the β-Ti-layer by diffusion of Cu. CuTi was predicted as the first phase to form in the diffusion zone, based on the MEHF model, which was followed by Cu_4Ti, Cu_4Ti_3 and $CuTi_2$ in that sequence.

The interdiffusion coefficients for Cu_4Ti and CuTi ($\tilde{D}_{Cu_4Ti}$ and $\tilde{D}_{CuTi}$) and integrated diffusion coefficient for Cu_4Ti_3 ($\tilde{D}^{int}_{Cu_4Ti_3}$) were evaluated. The diffusion parameters for interdiffusion in the compounds Cu_4Ti, Cu_4Ti_3 and CuTi were: $Q^{Cu_4Ti} = 192.2 \pm 3.4$ kJ mol^{-1}, $D_0^{Cu_4Ti} = 5.79^{+4.30}_{-2.49} \times 10^{-5}$ m^2 s^{-1}, $Q^{Cu_4Ti_3} = 209.2 \pm 4.3$ kJ mol^{-1}, $D_0^{Cu_4Ti_3} = 8.94^{+7.67}_{-4.12} \times 10^{-4}$ m^2 s^{-1}, $Q^{CuTi} = 187.7 \pm 3.2$ kJ mol^{-1} and $D_0^{CuTi} = 1.79^{+1.26}_{-0.74} \times 10^{-4}$ m^2 s^{-1}. The logarithm of interdiffusion coefficient ($\tilde{D}$) in the Cu(Ti) solid solution was found to decrease linearly with increase in C_{Ti} in the entire solubility range. The activation energy for interdiffusion in the Cu(Ti) solid solution varied linearly between 201.0 kJ mol^{-1} and 247.5 kJ mol^{-1} within the composition range C_{Ti} = 0.5–4.0 at.% Ti. The impurity diffusion coefficient of Ti in pure Cu, evaluated by extrapolation of $\tilde{D}$ to infinite dilution ($C_{Ti} \approx 0$), showed a temperature dependence: $D_{Ti}^{Cu} = 9.92 \times 10^{-5} \exp\left(\frac{-200.2 \text{ kJ mol}^{-1}}{RT}\right)$ m^2 s^{-1}. The values of D_{Ti}^{Cu} were found to be consistent with the general theories of impurity diffusion.

The authors are grateful to Dr. G. K. Dey, Head, Materials Science Division, Bhabha Atomic Research Centre, for his keen interest, support and encouragement in the present work.

References

[1] I.S. Batra, G.K. Dey, U.D. Kulkarni, S. Banerjee: Mater. Sci. Eng. A 360 (2003) 220. DOI:10.1016/S0921-5093(03)00440-4
[2] W.R. Osório, A. Cremasco, P.N. Andrade, A. Garcia, R. Caram: Electrochim. Acta 55 (2010) 759. DOI:10.1016/j.electacta.2009.09.016
[3] A. Meier, P.R. Chidambaram, G.R. Edwards: Acta Mater. 46 (1998) 4453. DOI:10.1016/S1359-6454(98)00100-1
[4] C. Borchers: Phil. Mag. A 79 (1999) 537. DOI:10.1080/01418619908210315
[5] F.H. Santiago, N.C. Castro, V.M.L. Hirata, H.J.D. Rosales, J.D.J.C. Rivera: Mater. Trans. 45 (2004) 2312. DOI:10.2320/matertrans.45.2312
[6] U.D. Kulkarni, G.K. Dey, I.S. Batra: Metall. Mater. Trans. A 33 (2002) 3573. DOI:10.1007/s11661-002-0346-4
[7] J. Rexer: Z. Metallkd. 63 (1972) 745.
[8] O. Taguchi, Y. Iijima, K. Hirano: J. Jpn. Inst. Met. 54 (1990) 619.
[9] Y. Iijima, K. Hoshino, K. Hirano: Metall. Trans. A 8 (1977) 997.
[10] V.E. Oliker, A.A. Mamonova, T.I. Shaposhnikova: Powder Metall. Met. Ceram. 35 (1996) 173. DOI:10.1007/BF01389606
[11] A.E. Gershinskii, A.A. Khoromenko, E.I. Cherepov: Phys. Status Solidi A 31 (1975) 61. DOI:10.1002/pssa.2210310107

[12] J.L. Liotard, D. Gupta, P.A. Psaras, P.S. Ho: J. Appl. Phys. 57 (1985) 1895. DOI:10.1063/1.334422
[13] J. Andrieux, O. Dezellus, F. Bosselet, J.C. Viala: J. Phase Equilib. Diffus. 30 (2009) 40. DOI:10.1007/s11669-008-9424-7
[14] R.K. Shiue, S.K. Wu, C.H. Chan: J. Alloys Compd. 372 (2004) 148. DOI:10.1016/j.jallcom.2003.09.155
[15] D.E. Laughlin, J.W. Cahn: Acta Metall. 23 (1975) 329. DOI:10.1016/0001-6160(75)90125-X
[16] D.E. Laughlin, J.W. Cahn: Metall. Trans. 5 (1974) 972. DOI:10.1007/BF02643164
[17] A. Datta, W. Soffa: Acta Metall. 24 (1976) 987. DOI:10.1016/0001-6160(76)90129-2
[18] M.R. Bateni, S. Mirdamadi, F. Ashrafizadeh, A. Szpunar, R.A.L. Drew: Mater. Manuf. Proc. 16 (2001) 219. DOI:10.1081/AMP-100104302
[19] H. Okamoto: J. Phase Equilib. 26 (2002) 549. DOI:10.1361/105497102770331307
[20] P. Canale, C. Servant: Z. Metallkd. 93 (2002) 273.
[21] J.L. Murray: in: T. B. Massalski, H. Okamoto, P. R. Subramanian, L. Kacprzak (Eds.), Binary Alloy Phase Diagrams, ASM International, Materials Park, Ohio (1990) 1494–1496.
[22] A. Ouensanga: J. Less-Common Met. 79 (1981) 237. DOI:10.1016/0022-5088(81)90072-2
[23] J.L. Pouchou, F. Pichoir: Microbeam Analysis, San Francisco Press, San Francisco, CA (1988) pp. 315–318.
[24] K. Bhanumurthy, G.B. Kale, S.K. Khera: Metall. Trans. A 23 (1992) 1373.
[25] O. Taguchi, Y. Iijima, K. Hirano: J. Alloy Compd. 215 (1994) 329. DOI:10.1016/0925-8388(94)90862-1
[26] G.P. Tiwari, Y. IIjima, G.B. Kale: Diffus. Defect Data, Pt. A 279 (2008) 117.
[27] J. Andrieux, O. Dezellus, F. Bosselet, M. Sacerdote-Peronnet, J.C. Viala: XXXII JEEP (2006).
[28] J. Andrieux, O. Dezellus, F. Bosselet, M. Sacerdote-Peronnet, C. Sigala, R. Chiriac, J.C. Viala: J. Phase Equilib. Diffus. 29 (2008) 156. DOI:10.1007/s11669-008-9247-6
[29] A. Laik, K. Bhanumurthy, G.B. Kale: Intermetallics 12 (2004) 69. DOI:10.1016/j.intermet.2003.09.002
[30] F.J.J. van Loo: Prog. Solid State Chem. 20 (1990) 47. DOI:10.1016/0079-6786(90)90007-3
[31] V.I. Dybkov: Reaction Diffusion and Solid State Chemical Kinetics IPMS Publication, Kyiv (2002).
[32] R.M. Walser, R.W. Bené: Appl. Phys. Lett. 28 (1976) 624. DOI:10.1063/1.88590
[33] B.Y. Tsaur, S.S. Lau, J.W. Mayer, M.A. Nicolet: Appl. Phys. Lett. 38 (1981) 922. DOI:10.1063/1.92183
[34] R.W. Bené: Appl. Phys. Lett. 41 (1982) 529. DOI:10.1063/1.93578
[35] M. Ronay: Appl. Phys. Lett. 42 (1983) 577. DOI:10.1063/1.94007
[36] R. Pretorius: MRS Proc. 25 (1984) 15. DOI:10.1557/PROC-25-15
[37] R. Pretorius, R. de Reus, A.M. Vredenberg, F.W. Saris: J. Appl. Phys. 70 (1991) 3636. DOI:10.1063/1.349211
[38] R. Pretorius, T.K. Marais, C.C. Theron: Mater. Sci. Eng., R 10 (1993) 1.
[39] K. Bhanumurthy, G.B. Kale, S.P. Garg: Trans. Ind. Inst. Metals 48 (1995) 193.
[40] K.C. Hari Kumar, I. Ansara, P. Wollants, L. Delaey: Z. Metallkd. 87 (1996) 666.
[41] C. Colinet, A. Pasturel, K.H.J. Buschow: J. Alloys Compd. 247 (1997) 15. DOI:10.1016/S0925-8388(96)02590-X
[42] G. Ghosh: Acta Mater. 55 (2007) 3347. DOI:10.1016/j.actamat.2007.01.037
[43] L. Kaufman, H. Bernstein: Computer calculations of phase diagrams, Academy Press, New York (1970).
[44] N. Saunders, A.P. Miodownik: CALPHAD (Calculation of Phase Diagrams): A comprehensive guide, 1st ed., Pergamon Press, New York (1998).
[45] A.T. Dinsdale: CALPHAD 15 (1991) 317. DOI:10.1016/0364-5916(91)90030-N
[46] L. Boltzmann: Annal. Phys. 53 (1894) 959. DOI:10.1002/andp.18942891315
[47] C. Matano: Jpn. J. Phys. 8 (1933) 109.
[48] T. Heumann: Z. Phys. Chem. 201 (1952) 168.
[49] R.W. Balluffi: Acta Metall. 8 (1960) 871. DOI:10.1016/0001-6160(60)90154-1
[50] P. Villars, L.D. Calvert: Pearson's Handbook of Crystallographic Data for Intermetallic Phases, vol. 2, ASM, Metals Park, Ohio (1985).
[51] W.B. Krull, R.W. Newman: J. Appl. Crystall. 3 (1970) 519. DOI:10.1107/S0021889870006787
[52] M.A. Dayananda: Diffus. Defect Data, Pt. A 95 – 98 (1993) 521.
[53] C. Wagner: Acta Metall. 17 (1969) 99. DOI:10.1016/0001-6160(69)90131-X
[54] R.C. Ecob, J.V. Bee, B. Ralph: Phys. Status Solidi A 52 (1979) 201. DOI:10.1002/pssa.2210520121
[55] J.Y. Brun, S. Hamar-Thibault, C. Allibert: Z. Metallkd. 74 (1983) 525.
[56] N. Karlsson: J. Inst. Met. 79 (1951) 391.
[57] F. Sauer, V. Freise: Z. Electrochem. 66 (1962) 353.
[58] L.D. Hall: J. Chem. Phys. 21 (1953) 87. DOI:10.1063/1.1698631
[59] H. Mehrer: Diffusion in Solids, Springer-Verlag, Berlin (2007).
[60] S. Nagarjuna, M. Srinivas, K. Balasubramanian, D.S. Sarma: Mater. Sci. Eng. A 259 (1999) 34. DOI:10.1016/S0921-5093(98)00882-X
[61] W.F. Gale, T.C. Totemeier: Smithells Metals Reference Book, chap. Diffusion, 8th ed., Butterworth, Oxford (2004) .
[62] A.D. Le Claire: Phil. Mag. 7 (1962) 141. DOI:10.1080/14786436208201866
[63] A.D. Le Claire: in: H. Eyring, D. Henderson, W. Jost (Eds.), Physical Chemistry – An Advanced Treatise, vol. X, Academic Press, New York and London (1970) 261–330.
[64] G. Neumann, C. Tuijn: Self Diffusion and Impurity Diffusion in Pure Metals: Handbook of Experimental Data, vol. 14 of Pergamon Materials Series, Elsevier Ltd. (2009).
[65] C. Zener: J. Appl. Phys. 22 (1951) 372. DOI:10.1063/1.1699967
[66] R.A. Swalin: J. Appl. Phys. 27 (1956) 544. DOI:10.1063/1.1722421
[67] D. Beke, T. Geszti, G. Erdelyi: Z. Metallkd. 68 (1977) 444.
[68] D. Lazarus: Phys. Rev. 93 (1954) 973. DOI:10.1103/PhysRev.93.973
[69] J. Pelleg: Acta Metall. 14 (1966) 229. DOI:10.1016/0001-6160(66)90306-3

(Received September 15, 2010; accepted December 3, 2011)

Bibliography

DOI 10.3139/146.110685
Int. J. Mat. Res. (formerly Z. Metallkd.)
103 (2012) 6; page 661 – 672

ISSN 1862-5282

Correspondence address

Arijit Laik
Materials Science Division
Bhabha Atomic Research Centre
Mumbai 400 085, India
Tel.: +91 22 2559 0457
Fax: +91 22 2550 5151
E-mail: laik@barc.gov.in

You will find the article and additional material by entering the document number **MK110685** on our website at *www.ijmr.de*